

Research Articles | Behavioral/Cognitive

## Superagers resist typical age-related white matter structural changes

<https://doi.org/10.1523/JNEUROSCI.2059-23.2024>

Received: 2 November 2023

Revised: 10 January 2024

Accepted: 31 January 2024

Copyright © 2024 Garo-Pascual et al.

This is an open-access article distributed under the terms of the [Creative Commons Attribution 4.0 International license](#), which permits unrestricted use, distribution and reproduction in any medium provided that the original work is properly attributed.

---

*This Early Release article has been peer reviewed and accepted, but has not been through the composition and copyediting processes. The final version may differ slightly in style or formatting and will contain links to any extended data.*

**Alerts:** Sign up at [www.jneurosci.org/alerts](http://www.jneurosci.org/alerts) to receive customized email alerts when the fully formatted version of this article is published.

1 **Title: Superagers resist typical age-related white matter structural changes**

2 **Abbreviated title:** White matter structure of superagers

3 **Authors and affiliations:** Marta Garo-Pascual<sup>1,2,3\*</sup>, Linda Zhang<sup>2</sup>, Meritxell Valentí-Soler<sup>2</sup>,  
4 Bryan A. Strange<sup>1,2\*</sup>

5 <sup>1</sup>Laboratory for Clinical Neuroscience, Centre for Biomedical Technology, Universidad  
6 Politécnica de Madrid, IdISSC, Madrid, Spain 28223

7 <sup>2</sup>Alzheimer Disease Research Unit, CIEN Foundation, Queen Sofia Foundation Alzheimer  
8 Centre, Madrid, Spain 28031

9 <sup>3</sup>PhD Program in Neuroscience, Autonomous University of Madrid-Cajal Institute, Madrid,  
10 Spain 28029

11 **\*Corresponding authors:** marta.garo@ctb.upm.es (M. Garo-Pascual) and  
12 bryan.strange@upm.es (B.A. Strange)

13 Pages 37, figures 3 and table 1, abstract 250 words, significance statement 120 words,  
14 introduction 621 words and discussion 1491 words.

15 **Conflict of interest statement:** The authors declare no competing financial interest.

16 **Acknowledgments:** We thank the participants of the Vallecas Project and the staff of the  
17 CIEN Foundation. This work was supported by the CIEN Foundation and the Queen Sofia  
18 Foundation, as well as by a grant from the Spanish Ministry of Science and Innovation  
19 (PID2020-119302RB-I00) to BAS. MGP was supported by a MAPFRE-Queen Sofia  
20 Foundation scholarship. LZ was supported by a grant from the Alzheimer's Association (2016-  
21 NIRG-397128) to BAS.

22

23 **ABSTRACT**

24 Superagers are elderly individuals with the memory ability of people 30 years younger and  
25 provide evidence that age-related cognitive decline is not inevitable. In a sample of 64  
26 superagers (mean age 81.9; 59% women) and 55 typical older adults (mean age 82.4; 64%  
27 women) from the Vallecas Project, we studied, cross-sectionally and longitudinally over 5 years  
28 with yearly follow-ups, the global cerebral white matter status as well as region-specific white  
29 matter microstructure assessment derived from diffusivity measures. Superagers and typical  
30 older adults showed no difference in global white matter health (total white matter volume,  
31 Fazekas score, and lesions volume) cross-sectionally or longitudinally. However, analyses of  
32 diffusion parameters revealed better white matter microstructure in superagers than in typical  
33 older adults. Cross-sectional differences showed higher fractional anisotropy (FA) in  
34 superagers mostly in frontal fibres and lower mean diffusivity (MD) in most white matter tracts,  
35 expressed as an anteroposterior gradient with greater group differences in anterior tracts. FA  
36 decrease over time is slower in superagers than in typical older adults in all white matter tracts  
37 assessed, which is mirrored by MD increases over time being slower in superagers than in  
38 typical older adults in all white matter tracts except for the corticospinal tract, the uncinate  
39 fasciculus and the forceps minor. The better preservation of white matter microstructure in  
40 superagers relative to typical older adults supports resistance to age-related brain structural  
41 changes as a mechanism underpinning the remarkable memory capacity of superagers, while  
42 their regional ageing pattern is in line with the last-in-first-out hypothesis.

43

44

45

46

47 **SIGNIFICANCE STATEMENT**

48 Episodic memory is one of the cognitive abilities most vulnerable to ageing. Although memory  
49 normally declines with age, some older people may have memory performance similar to that  
50 of people 30 years younger, and this phenomenon is often conceptualised as superageing.  
51 Understanding the superager phenotype can provide insights into mechanisms of protection  
52 against age-related memory loss and dementia. We studied the white matter structure of a  
53 large sample of 64 superagers over the age of 80 and 55 age-matched typical older adults  
54 during 5 years with yearly follow-ups showing evidence of slower age-related changes in the  
55 brains of superagers especially in protracted maturation tracts, indicating resistance to age-  
56 related changes and a regional ageing pattern in line with the last-in-first-out hypothesis.

57

58

59

60

61

62

63

64

65

66

67

## 68 INTRODUCTION

69 Ageing is a dynamic process involving functional and structural brain changes. One of the  
70 cognitive functions most vulnerable to ageing is episodic memory, the ability to retrieve our  
71 personal experiences (Glisky, 2007). Pathological deterioration of episodic memory is a feature  
72 of Alzheimer's disease, the leading cause of dementia. Yet episodic memory can also be  
73 robust to age-related changes and this phenomenon has been conceptualised and studied  
74 under the definition of "superagers". Superagers are older adults with the episodic memory of  
75 a healthy adult 20-30 years younger (Cook et al., 2017; Gefen et al., 2015; Harrison et al.,  
76 2018; Harrison et al., 2012; Sun et al., 2016). Structural and functional neuroanatomical  
77 characterisation of superagers may reveal the neural substrates of successful episodic  
78 memory ageing and, thus, provide insight into how it is possible to age without episodic  
79 memory impairment. In this study we focused on structural parameters of white matter health  
80 to extend our previous work on the grey matter signature of a group of superagers from the  
81 Vallecas Project cohort (Garo-Pascual et al., 2023).

82 White matter undergoes changes with ageing, white matter volume decreases, microstructural  
83 properties are lost, and lesions accumulate (Cox et al., 2016; Davis et al., 2009; de Leeuw et  
84 al., 2001; Westlye et al., 2010; Ylikoski et al., 1995). These changes are regionally  
85 heterogeneous, being greater in anterior than posterior brain regions (Davis et al., 2009;  
86 Kochunov et al., 2007; O'Sullivan et al., 2001; Pfefferbaum et al., 2005; Sullivan and  
87 Pfefferbaum, 2006). This occurs in conjunction with changes of white matter microstructural  
88 properties in the thalamic radiations and association fasciculi (Cox et al., 2016; Slater et al.,  
89 2019). This white matter ageing pattern inverts the sequence of myelination early in life and  
90 supports the last-in-first-out hypothesis (Raz, 2000) since white matter tracts that first  
91 experience the effects of ageing, like the thalamic radiations and association fibres, also show  
92 protracted maturation in early life.

93 White matter loss with ageing is associated with worsening cognitive performance affecting  
94 processing speed, primarily impairing executive functions (Kennedy and Raz, 2009; Tubi et  
95 al., 2020). Episodic memory function in the cognitively healthy elderly is also negatively  
96 associated with white matter microstructural properties of the uncinate, inferior and superior  
97 longitudinal fasciculus, thalamic radiations, and dorsal cingulum bundle (Lockhart et al., 2012;  
98 Sasson et al., 2013; Ziegler et al., 2010). White matter microstructure has already been studied  
99 in cohorts of successful episodic memory agers, specifically in cohorts between 60-80yo,  
100 showing better properties in superagers in the corpus callosum and the right superior  
101 longitudinal fasciculus (Kim et al., 2020).

102 We studied the brain white matter status and white matter microstructure proxies in a sample  
103 of 64 superagers and 55 typical older adults that are over 80yo to characterise brain white  
104 matter in an older age range of superagers that is, to our knowledge, currently unexplored. We  
105 approached this study with a cross-sectional and longitudinal characterisation of 1) global  
106 white matter status and 2) white matter microstructure derived from diffusion tensor imaging  
107 parameters. In our previous study, which characterised grey matter volumes of the same  
108 sample of superagers compared to typical older adults (Garo-Pascual et al., 2023), we  
109 concluded that superagers express a resistance to age-related brain changes as manifested  
110 in greater grey matter volume and slower atrophy in the medial temporal lobe and motor  
111 thalamus compared to typical older adults. In the current study, we hypothesised that the  
112 superager brain would show resistance to age-related white matter changes and would have  
113 better global white matter status and preserved white matter microstructure –higher fractional  
114 anisotropy (FA) and lower mean diffusivity (MD)– in anterior tracts especially the anterior  
115 thalamic radiation and association fibres in comparison to typical older adults as these are the  
116 more vulnerable tracts to age-related changes.

117

## 118 MATERIALS AND METHODS

119 **Participants.** The sample of superagers and typical older adults used in this study were  
120 selected from the single-centre community based Vallecas Project, an ongoing longitudinal  
121 cohort established in Madrid (Spain). The 1,213 participants of the Vallecas Project were all of  
122 Caucasian ethnicity, community-dwelling individuals between 70 to 85 years-old, independent  
123 in activities of daily living with a survival expectancy of at least 4 years and without any  
124 neurological or psychiatric disorders (Olazarán et al., 2015). All participants provided written  
125 informed consent, and the project was approved by the Ethics Committee of the Instituto de  
126 Salud Carlos III. We applied criteria for superagers and typical older adults to the Vallecas  
127 Project cohort based on the definition of a superager as a person aged 80 years or older with  
128 the episodic memory of a person 20-30 years younger. The selection criteria for this analysis  
129 focused on five aspects including age, episodic memory performance, cognitive performance  
130 in non-memory domains, availability of MRI scans, and stability of episodic memory. Both  
131 candidates for the superager and the typical older adult group were 79.5 years or older when  
132 their episodic memory was screened with the free delayed recall score on the verbal memory  
133 free and cued selective reminding test. For participants to be considered as superagers they  
134 were required to perform at or above the mean of the score of adults aged 50-56 years with  
135 the same education attainment and typical older adults were required to score within one  
136 standard deviation from the mean of the normative values for their age and education  
137 attainment in the Spanish NEURONORMA project (Peña-Casanova et al., 2009). Complete  
138 details on the selection of superagers and typical older adults from the Vallecas project are  
139 described elsewhere (Garo-Pascual et al., 2023).

140 **MRI data acquisition.** MRI images were acquired using a 3 Tesla MRI (Sigma HDxt GEHC,  
141 Waukesha, USA) with a phased array 8 channel head coil. T1-weighted images (3D fast  
142 spoiled gradient echo with inversion recovery preparation) were collected using a TR of 10ms,  
143 TE of 4.5ms, FOV of 240mm and a matrix size of 288x288 with slice thickness of 1mm, yielding

144 a voxel size of 0.5 x 0.5 x 1 mm. Diffusion-weighted images were single-shot SE-EPI, with TR  
145 9200ms, TE 80ms, b-value 800s/mm<sup>2</sup> and 21 gradient directions, FOV 240mm and matrix size  
146 128 x 128 with slice thickness of 3mm. T2-FLAIR (image attenuated inversion recovery)  
147 images were acquired with TR 9000 ms, TE 130 ms, TI 2100 ms, FOV 24 mm, slice thickness  
148 3.4 mm.

149 **Brain white matter volume and white matter lesions volume.** Brain white matter volume  
150 and white matter lesions volume were extracted from the segmentation of T1-weighted images  
151 using CAT12.7 toolbox (<https://neuro-jena.github.io/cat>) implemented in SPM12 (version  
152 r6225; <https://www.fil.ion.ucl.ac.uk/spm>) (Ashburner and Friston, 2005). This pipeline was run  
153 for cross-sectional and longitudinal analyses, with the latter including scans from visit 1 to visit  
154 6. Total intracranial volume (TIV) was also extracted using this protocol for analytical purposes  
155 as a covariate. White matter lesions are typically detected as hyperintense radiological  
156 observations in T2-FLAIR images. Here, however, we computed the volume of white matter  
157 lesions from T1-weighted images using the CAT12 toolbox, which provides a similar  
158 performance compared to existing methods of white matter hyperintensity detection from T2-  
159 FLAIR data (Dahnke et al., 2019).

160 **Fazekas score.** The Fazekas scale (Fazekas et al., 1987) quantifies brain white matter  
161 hyperintensities from MRI data with a scale as 0 = absence, 1 = focal lesions, 2 = start of  
162 confluent lesions and 3 = diffuse affection in a region ± U-shaped fibres. For our cohort, the  
163 lesions were graded by a radiologist blinded to the subject's group using T2-FLAIR images.

164 **White matter tract-based spatial statistics (TBSS) of diffusivity measures.** For  
165 preprocessing of diffusion-weighted images, FSL was used (<http://fsl.fmrib.ox.ac.uk/fsl/fslwiki>)  
166 and the pipeline included a motion and eddy current correction, the extraction of non-brain  
167 voxels and ends with the calculation of voxel-wise diffusion maps —FA and MD— for each  
168 participant. Both FA and MD are derived from the eigenvalues of the diffusion tensor captured



169 by diffusion-weighted images; FA measures the directionality of water diffusion, while MD  
170 averages the diffusivity of water molecules in the three directions of the space reflecting tissue  
171 constraints. Individual diffusion maps were then used in the TBSS pipeline using the FMRIB  
172 toolbox (<http://fsl.fmrib.ox.ac.uk/fsl/fslwiki>) (Smith et al., 2006). The general outline of the  
173 process is 1) FA individual maps were non-linearly registered to standard space (FMRIB58\_FA  
174 template) (Andersson et al., 2007); 2) a mean FA image was created by averaging all co-  
175 registered FA maps; and 3) individually aligned images were projected onto the mean FA  
176 skeleton, representing the centres of all tracts common to the study sample (visual inspection  
177 was required to set a threshold of mean FA at 0.25 to include non-skeleton voxels) and  
178 skeletonised images were used for voxel-wise analysis. Diffusivity maps for MD were  
179 generated by applying the same steps detailed above. For cross-sectional analysis, diffusivity  
180 maps for FA and MD were entered into separate general linear models (GLM) to compare  
181 differences between the superager and the control group. TIV, age, gender and years of  
182 education were used as covariates. We conducted whole-brain analyses using a Threshold  
183 Free Cluster Enhancement (TFCE) approach with 5000 permutations (default parameters  $E =$   
184  $0.5$  and  $H = 2$ ). Significant results are reported at a FWE-corrected level of  $P < 0.05$ . To  
185 visualise our results we used the multimodal analysis and visualisation tool (MMVT)  
186 (Felsenstein et al., 2019). The same preprocessing pipeline and GLM was built for additional  
187 diffusivity measures including mode of anisotropy, axial and radial diffusivity (Figure 1-2). While  
188 MD averages the diffusivity of water molecules in the three directions of the space, axial  
189 diffusivity reflects the diffusion of water molecules in the parallel orientation to the axonal  
190 bundle and radial diffusivity averages the two perpendicular diffusivity directions. Mode of  
191 anisotropy is mathematically orthogonal to FA and reflects the geometrical properties of the  
192 directionality of water diffusion (i.e., linear, or planar directionality). FA and MD values were  
193 also explored longitudinally replicating with longitudinal scans the same preprocessing steps  
194 described above and further used for a regions of interest (ROI)-based analysis conducted by  
195 averaging the FA and MD values from 18 ROIs described in the JHU-ICBM thr25 atlas (Hua

196 et al., 2008; Wakana et al., 2007) (Figure 3-1, Figure 3-2). The statistical model is specified in  
197 the statistical analysis section.

198 **Longitudinal diffusivity analysis in SPM.** Whole-brain voxel-wise analyses testing  
199 longitudinal group differences in two measures derived from diffusion-weighted imaging  
200 sequences —FA and MD— were carried out using SPM12 (version r6225;  
201 <https://www.fil.ion.ucl.ac.uk/spm>) and FSL (<https://fsl.fmrib.ox.ac.uk/fsl/fslwiki/>) (Jenkinson et  
202 al., 2012). The preprocessing of diffusion-weighted images was conducted in FSL as described  
203 in the previous section. We performed eddy current correction, brain segmentation to exclude  
204 non-brain voxels and calculation of FA and MD parameters with the FMRIB toolbox  
205 (<https://fsl.fmrib.ox.ac.uk/fsl/fslwiki/>). The resulted FA and MD maps were normalised to  
206 standardise Montreal Neurological Institute (MNI) space using the TBSS pipeline (Smith et al.,  
207 2006), a non-linear registration to set individual's maps into the standard template  
208 FMRB58\_FA. *Randomise*, the FSL function that builds GLM, does not support reliable  
209 longitudinal analysis, so the preprocessed data was further analysed in SPM similarly to  
210 previous authors (Lei et al., 2012).

211 The normalised FA and MD maps generated in FSL were then smoothed in SPM12 using a 6  
212 mm FWHM Gaussian kernel. In the longitudinal toolbox in CAT12, separate GLM models were  
213 specified for FA and MD. Age at each MRI acquisition was included as a covariate interacting  
214 with the group factor. A masking threshold of 0.1 was applied to FA images to remove effects  
215 out of the brain. No masking threshold was used in MD images since the MD values have a  
216 low order of magnitude. These voxel-wise analyses were conducted using TFCE approach  
217 with 5000 permutations and default parameters ( $E = 0.5$  and  $H = 2$ ) using the TFCE tool  
218 (version r223) from CAT12 toolbox in SPM12 (<https://www.neuro.uni-jena.de/tfce>). Significant  
219 results are reported at FWE-corrected level of  $P < 0.05$ . The neuroanatomical loci were  
220 reported according to the Mori and the JHU-ICBM thr25 atlas (Hua et al., 2008; Wakana et al.,  
221 2007) and Mango software (<http://rui.uthscsa.edu/mango/>) was used to produce the figure.

222 **Statistical analysis.** Cross-sectional group comparisons for white matter volume and white  
223 matter lesions volume were conducted with an analysis of covariance with TIV as covariate.  
224 Categorical data was evaluated with a Chi-squared test or Fisher exact test. Differences in the  
225 longitudinal trajectories of neuropsychological variables, white matter volume, white matter  
226 lesions volume and Fazekas scores (computed as numeric due to the accumulative nature of  
227 the scale) and ROI-based FA and MD values were studied with a linear mixed effects model  
228 built with the lme4 package in R (Bates et al., 2015). In these linear mixed effects models,  
229 white matter volume and white matter lesions volume were adjusted by TIV; scaled age, group  
230 and the interaction between scaled age and group were the fixed factors; and the random  
231 intercept and the random slope were included. We excluded from the longitudinal analysis of  
232 white matter lesions volume four outliers (three typical older adults and a superager) informed  
233 by the Bonferroni outlier test of the car package in R (Fox and Weisberg, 2019) that considers  
234 the longitudinal trajectory of the linear mixed effects model. Group differences in the  
235 anteroposterior gradient of MD were explored in the cross-sectional analysis. The brain map  
236 of the unthresholded parameter estimates ( $\beta$ ) of the comparison MD in typical older adults  
237 minus MD in superagers was sliced in the coronal plane every 5mm in the anteroposterior axis  
238 creating 31 slices. We then estimated the average  $\beta$  in each slice and fit a linear regression to  
239 this value as a function of the anteroposterior axis Montreal Neurologic Initiative (MNI)  
240 coordinates. Whole brain significant results are reported at a TFCE corrected threshold as  
241 described above. Significant results are reported at a false discovery rate (FDR) corrected  
242 level of  $P < 0.05$ . All statistical analysis described were performed in R 4.0.2 ([https://www.r-](https://www.r-project.org/)  
243 [project.org/](https://www.r-project.org/)).

244

245

246

## 247 RESULTS

248 A sample of 64 superagers and 55 typical older adults were identified in the Vallecas Project  
249 cohort with no significant differences in age or sex (Table 1). Superagers outperformed typical  
250 older adults in the neuropsychological selection criteria variables (Table 1), however their  
251 longitudinal evaluation showed no significant group by time interaction in the free delay recall  
252 score of the free and cued selective reminding test ( $t(1, 597) = 1.60, P = 0.11$ ), the digit symbol  
253 substitution test ( $t(1, 478) = 0.86, P = 0.40$ ) and the 15-item Boston naming test ( $t(1, 482) =$   
254  $1.32, P = 0.19$ ), whereas the significant group by time interaction in the animal fluency test  
255 ( $t(1, 600) = 2.13, P = 0.03$ ) indicates a slower decline in superagers compared to typical older  
256 adults (Table 1-1).

257 White matter status of superagers and typical older adults was compared cross-sectionally and  
258 longitudinally over five years using three parameters to assess the general status of white  
259 matter: 1) total brain white matter volume, 2) volume of white matter lesions extracted  
260 automatically from T1-weighted images and 3) the Fazekas score (Fazekas et al., 1987), a  
261 radiological scale for quantifying the amount of white matter T2 hyperintense lesions (see  
262 Methods). This general white matter status assessment was complemented with a regionally  
263 specific approach to test for voxel-wise group cross-sectional and longitudinal differences in  
264 two diffusivity measures, FA and MD.

### 265 **Cross-sectional white matter structural differences between superagers and typical** 266 **older adults**

267 Superagers and typical older adults showed no cross-sectional differences in total white matter  
268 volume ( $F(1, 115) = 0.4, P = 0.54$ ) (Table 1) or in the volume of white matter lesions ( $F(1, 115)$   
269  $= 2.0, P = 0.17$ ) (Table 1). The Fazekas scores revealed that a similar proportion of superagers  
270 (85.9%) and typical older adults (83.3%) have white matter T2 hyperintense lesions ( $\chi = 0.02,$   
271  $P = 0.89$ ) (Table 1). This high prevalence of white matter lesions is in accordance with

272 observations from other elderly cohorts (American Psychiatric Association, 1994; de Leeuw et  
273 al., 2001). There were no between-group differences in the degree of these lesions ( $P = 0.45$ )  
274 (Table 1). We observed a significant correlation between white matter lesion volume and the  
275 Fazekas score (Pearson's  $r = 0.73$ ,  $P < 0.0001$ ).

276 We next adopted a regionally specific approach to test for cross-sectional voxel-wise group  
277 differences in FA and MD. Better white matter microstructure in terms of diffusivity translates  
278 into higher FA and lower MD values. We observed higher FA in superagers than typical older  
279 adults mainly in frontal regions of the inferior fronto-occipital fasciculus, anterior thalamic  
280 radiation, right inferior longitudinal fasciculus, right forceps minor and left forceps major ( $P <$   
281  $0.05$  FWE-corrected) (Figure 1A). Lower MD values were found in superagers compared to  
282 typical older adults in an extensive network comprising the forceps major and minor, superior  
283 and inferior longitudinal fasciculus, inferior fronto-occipital fasciculus, anterior thalamic  
284 radiation, and cingulum bundle ( $P < 0.05$  FWE-corrected) (Figure 1B). The anteroposterior  
285 gradient of these group effects (higher MD in typical older adults than superagers) was tested  
286 by fitting a linear regression model of the parameter estimate ( $\beta$ ) of this contrast as a function  
287 of anteroposterior axis coordinates. We observed a significant effect ( $\beta$  ( $t(29) = 5.31$ ,  $P <$   
288  $0.0001$ )) supporting stronger MD group differences in the anterior portion of the brain (Figure  
289 1B). The average FA and MD values of the significant clusters in the voxel-wise group contrast  
290 were correlated with the episodic memory performance in the free and cued selective  
291 reminding test (Figure 1-1). Additional diffusivity measures including axial and radial diffusivity  
292 and mode of anisotropy were explored (Figure 1-2) and support the above results of superior  
293 white matter microstructural properties in the superager brain.

294 **Longitudinal white matter structural differences between superagers and typical older**  
295 **adults**

296 Longitudinal assessment of white matter structure, both for the general status metrics and for  
297 the regional approach on FA and MD, was performed over 5 years with yearly follow-ups  
298 (median number of follow-up visits was 5.0 (IQR 5.0-6.0) for superagers and 5.0 (4.5-6.0) for  
299 typical older adults). The longitudinal evolution of total white matter volume suggest similar  
300 atrophy rates in superagers and typical older adults as the group by time interaction is not  
301 significant ( $t(1, 578) = 0.2, P = 0.81$ ) (Figure 2, Figure 2-1). The longitudinal load of white matter  
302 lesions volume over time is significantly slower in superagers compared to typical older adults  
303 ( $t(1, 578) = 2.4, P = 0.02$ ) but this group by time interaction did not survive the exclusion of  
304 outliers (three typical older adults and a superager) ( $t(1,558) = 1.6, P = 0.11, \beta(\text{SE})$  superager:  
305 0.69 (0.14),  $\beta(\text{SE})$  typical older adult: 1.01 (0.15)) (Figure 2, Figure 2-1). The longitudinal  
306 evolution of lesions degree in the Fazekas scale revealed no between-group differences ( $t(1,$   
307  $578) = 0.3, P = 0.80$ ) (Figure 2-1). Thus, of the three global parameters assessed, no major  
308 differences in white matter status were found between superagers and typical older adults  
309 cross-sectionally or longitudinally.

310 Region-specific diffusivity measures were studied longitudinally over five years with yearly  
311 follow-up scans using a voxel-wise approach and complementary ROI-based analyses  
312 (extended data). We observed that FA decreases significantly slower in superagers compared  
313 to typical older adults in all white matter tracts described in the JHU-ICBM atlas (Figure 3), and  
314 diffuse but significant effects were found in the cingulum, hippocampal cingulum, and uncinate  
315 fasciculus bilaterally ( $P < 0.05$  FWE-corrected) (Figure 3A). ROI-based analyses yielded a  
316 significantly slower FA decrease in superagers compared to typical older adults in all white  
317 matter tracts assessed (Figure 3-1, Figure 3-2). The increase of MD over time was significantly  
318 slower in superagers compared to typical older adults in all tracts from the JHU-ICBM atlas  
319 with similar differences bilaterally and diffuse but significant effects in the cingulum ( $P < 0.05$   
320 FWE-corrected) (Figure 3B). ROI-based analyses revealed different group longitudinal  
321 trajectories in all white matter tracts except for the corticospinal tract, the uncinate fasciculus

322 and forceps minor (Figure 3-3, Figure 3-4). Altogether, these results indicate a resistance to  
323 age-related changes in white matter microstructure in superagers compared to typical older  
324 adults by showing a slower decrease of FA and a slower increase in MD over time.

325

326

327

328

329

330

331

332

333

334

335

336

337

338

339

340

## 341 **DISCUSSION**

342 Assessment of global cerebral white matter status indicated that superagers and typical older  
343 adults have similar white matter health cross-sectionally and longitudinally since no group  
344 differences were found in total brain white matter volume, white matter lesions volume and the  
345 Fazekas score. However, differences in diffusivity measures consistent with better white matter  
346 microstructure in superagers than typical older adults were found cross-sectionally and  
347 longitudinally. Cross-sectional differences show higher FA in superagers mostly in frontal fibres  
348 and lower MD in most white matter tracts following an anteroposterior gradient with greater  
349 group differences in anterior regions, both FA and MD values correlate with episodic memory  
350 performance in the whole sample. The decrease in FA over time is slower in superagers than  
351 typical older adults in all white matter tracts assessed and the increase of MD overtime is  
352 slower in superagers than typical older adults in all white matter tracts except for the  
353 corticospinal tract, the uncinate fasciculus and the forceps minor.

354 The regional study of diffusivity measures—FA and MD— confirms, firstly, better white matter  
355 microstructural properties in superagers than in typical older adults, both cross-sectionally and  
356 longitudinally, and, secondly, outlines regional brain patterns associated with ageing. Cross-  
357 sectionally, the greatest differences between groups for both FA and MD accumulate in the  
358 anterior part of the brain in line with the existing evidence that the anterior portion of the brain  
359 is more vulnerable to the effects of ageing (Davis et al., 2009; Kochunov et al., 2007; O'Sullivan  
360 et al., 2001; Pfefferbaum et al., 2005; Sullivan and Pfefferbaum, 2006). Although greater group  
361 differences in MD were found in the anterior areas, they were not constrained to the anterior  
362 portion like most FA effects. MD is a more sensitive parameter to age-related changes than  
363 FA (Cox et al., 2016), and this could explain its larger group differences. These marked group  
364 white matter differences in the anterior part of the brain, rather than the temporal, contrast with  
365 grey matter volume differences observed in medial temporal areas (Garo-Pascual et al., 2023).  
366 This result might suggest that the prefrontal cortex of superagers exerts more efficient top-



367 down control over medial temporal regions mediating more successful episodic memory  
368 function (Dobbins et al., 2002; Simons and Spiers, 2003; Szczepanski and Knight, 2014) by,  
369 for example, improving the retrieval of appropriate memories and suppressing the inappropriate  
370 ones (Anderson et al., 2016; Tomita et al., 1999).

371 Longitudinally, extensive group differences in white matter microstructure were found in most  
372 white matter tracts. However, ROI-based analysis revealed that MD trajectories over time were  
373 similar for both groups in the corticospinal tract, the uncinate fasciculus and the forceps minor.  
374 The absence of longitudinal differences between groups in the corticospinal tract and the  
375 forceps minor is of particular interest, as these are some of the most robust white matter tracts  
376 to the effects of ageing (Cox et al., 2016; Slater et al., 2019), supporting the last-in-first-out  
377 hypothesis (Raz, 2000). Therefore, the ageing trajectories between superagers and typical  
378 older adults mainly differ in association fibres and the anterior thalamic radiation—which are  
379 the most vulnerable to age-related changes (Cox et al., 2016; Slater et al., 2019)—reinforcing  
380 the idea that superagers exhibit a resistance mechanism to age-related changes (Garo-  
381 Pascual et al., 2023) and suggesting that the differential white matter status between groups  
382 has not been established in an early developmental stage. Indeed, longitudinal ROI-based FA  
383 and MD trajectories suggest equivalent values in both groups at around age 75, consistent  
384 with previous findings in grey matter volume (Garo-Pascual et al., 2023), at a time when  
385 superagers already outperformed typical older adults in episodic memory function. This  
386 suggests that the cognitive profile of superagers is established before reaching the criterion  
387 age and before structural brain differences are evident. The super-ageing phenotype may be  
388 dictated by a resistance versus a resilience mechanism, opposing concepts (Arenaza-Urquijo  
389 and Vemuri, 2018) that in the context of healthy ageing reflect as avoidance of age-related  
390 changes versus coping with age-related changes respectively (Garo-Pascual et al., 2023).  
391 Therefore, in brain structural terms, resistance to age-related changes translates into the better  
392 preservation of brain structure in superagers than in typical older adults consistent with our

393 white matter microstructural findings. Further evidence that resistance is the most plausible  
394 mechanism for superagers is its comparison with a group of middle-aged adults which, in our  
395 case, is not within the studied population demographic of the Vallecas Project cohort.

396 Fazekas scores revealed a high proportion of participants, whether superagers or typical older  
397 adults, with hyperintense white matter T2 lesions (~85%). Likewise, both groups experienced  
398 a longitudinal accumulation of white matter lesions, indexed by both the Fazekas scale and  
399 white matter lesion volume load, measures that were correlated in our sample. This high  
400 prevalence of white matter lesions is in line with observations from other elderly cohorts  
401 (American Psychiatric Association, 1994; de Leeuw et al., 2001), as is the increasing load of  
402 white matter lesions over time (Ylikoski et al., 1995). The correlation between the Fazekas  
403 scale and the volume of white matter lesions in our sample is also consistent with individuals  
404 in other elderly cohorts (Cedres et al., 2020; Valdes Hernandez Mdel et al., 2013; van Straaten  
405 et al., 2006). The absence of group differences in the prevalence and cumulative progression  
406 of white matter brain lesions reveals that these features are not only present in healthy ageing  
407 individuals but also occur in superageing. Superagers may be then showing resilience to white  
408 matter lesions in concurrence with resistance to age-related structural changes (including  
409 white matter microstructure and grey matter volume (Garo-Pascual et al., 2023)) as the primary  
410 protective ageing mechanism for maintenance of memory function.

411 The similar global white matter health between groups based on volumetric and radiological  
412 metrics contrasts with the better white matter microstructure of superagers relative to typical  
413 older adults observed on the regional study of diffusivity measures. This apparent discrepancy  
414 may have two explanations that are not mutually exclusive, the higher sensitivity of regional-  
415 based approaches over global measures and the differential ageing pattern of white matter  
416 volume and diffusivity measures. The white matter volume lifespan pattern exhibits an inverted  
417 U-shape peaking during the 5th-6th decade (Walhovd et al., 2011; Westlye et al., 2010), while  
418 diffusivity measures—including FA and MD—follow the same parabolic pattern but peak

419 around two decades earlier (Westlye et al., 2010). The time window in which we assessed our  
420 population is closer to the peak of white matter volume maturation than to the peak of diffusivity  
421 measures. Therefore, the shorter time between white matter volume maturation and our  
422 assessment could explain the similar group ageing trajectories despite finding a divergent  
423 ageing pattern in diffusivity measures.

424 White matter lesions (Haller et al., 2013) and age-related changes in white matter diffusion  
425 properties (Song et al., 2003; Song et al., 2005) underlie axonal and/or myelin degeneration  
426 yielding negative consequences for cognitive function (de Groot et al., 2000; Prins and  
427 Scheltens, 2015). The age-related accumulation of white matter lesions affects processing  
428 speed, mainly impairing executive function and, to a lesser extent, the memory domain (Prins  
429 and Scheltens, 2015; Tubi et al., 2020). Changes in white matter microstructure accounted by  
430 diffusivity measures have also a deleterious effect on memory performance (Goldstein et al.,  
431 2009). Poor white matter health has been associated with a vascular aetiology, as the  
432 prevalence of cardiovascular disease is a risk factor for the enlargement of white matter lesions  
433 (Debette and Markus, 2010; Launer et al., 2000) and the accumulation of vascular risk factors  
434 is associated with diffusivity parameters of impaired white matter microstructure (Ingo et al.,  
435 2021). Superagers showed lower prevalence of hypertension and glucose disorders than  
436 typical older adults (Garo-Pascual et al., 2023). However, they do not show differences in other  
437 cardiovascular risk factors (de Bruijn and Ikram, 2014) like high cholesterol, smoking status,  
438 obesity, diet—quantified as weekly frequency of food groups and adherence to Mediterranean  
439 diet—and physical activity (Garo-Pascual et al., 2023). Thus, the better white matter health in  
440 the brains of superagers relative to typical older adults could be explained by a higher burden  
441 of vascular risk factors in typical older adults, although not all cardiovascular risk factors  
442 support this speculation.

443 In summary, the better overall preservation of white matter microstructure in the brain of  
444 superagers supports resistance to age-related changes as their most plausible protective

445 mechanism for maintenance of memory function, in line with our previous results from  
446 structural analyses of grey matter of the superaging brain (Garo-Pascual et al., 2023). The  
447 regional ageing pattern identified a better preservation of white matter microstructural  
448 properties in superagers at the anterior portion of the brain and in those tracts with a protracted  
449 maturation which, according to the last-in-first-out hypothesis, are more vulnerable to age-  
450 related changes (Raz, 2000). The similar properties between superagers and healthy older  
451 adults in early developing white matter tracts may indicate that the superageing phenotype is  
452 not established during early development but is rather the result of a different ageing process  
453 in which vascular health might play an influential role.

454

455

456

457

458

459

460

461

462

463

464

465

466 **Author contributions:** MGP, LZ and BAS contributed to the conceptualisation of the study,  
467 MVS contributed with data curation, MGP and, LZ, contributed to the methodology and the  
468 investigation work of the study, BAS was responsible for the supervision of this work, MGP  
469 drafted the original manuscript and MGP, LZ, and BAS reviewed and edited the manuscript.

470 **Data sharing:** The Vallecas Project data collection is expected to be completed by the end of  
471 2023. Anonymised data can be accessed upon request at  
472 direccioncientifica@fundacioncien.es.

473

474

475

476

477

478

479

480

481

482

483

484

485

## 486 REFERENCES

- 487 American Psychiatric Association (1994). Diagnostic and statistical manual of mental  
488 disorders-IV (DSM-IV), 4th edn.
- 489 Anderson, M.C., Bunce, J.G., and Barbas, H. (2016). Prefrontal-hippocampal pathways  
490 underlying inhibitory control over memory. *Neurobiol Learn Mem* 134 Pt A, 145-161.
- 491 Andersson, J.L.R., Jenkinson, M., and Jenkinson, M. (2007). Non-linear registration, aka  
492 Spatial normalisation FMRIB Technical Report TR07JA2 (FMRIB Analysis Group of the  
493 University of Oxford).
- 494 Arenaza-Urquijo, E.M., and Vemuri, P. (2018). Resistance vs resilience to Alzheimer  
495 disease: Clarifying terminology for preclinical studies. *Neurology* 90, 695-703.
- 496 Ashburner, J., and Friston, K.J. (2005). Unified segmentation. *NeuroImage* 26, 839-851.
- 497 Bates, D., Mächler, M., Bolker, B., and Walker, S. (2015). Fitting Linear Mixed-Effects  
498 Models Using lme4. *Journal of Statistical Software* 67, 1 - 48.
- 499 Cedres, N., Ferreira, D., Machado, A., Shams, S., Sacuiu, S., Waern, M., Wahlund, L.O.,  
500 Zettergren, A., Kern, S., Skoog, I., *et al.* (2020). Predicting Fazekas scores from automatic  
501 segmentations of white matter signal abnormalities. *Aging (Albany NY)* 12, 894-901.
- 502 Cook, A.H., Sridhar, J., Ohm, D., Rademaker, A., Mesulam, M.M., Weintraub, S., and  
503 Rogalski, E. (2017). Rates of Cortical Atrophy in Adults 80 Years and Older With Superior vs  
504 Average Episodic Memory. *JAMA* 317, 1373-1373.
- 505 Cox, S.R., Ritchie, S.J., Tucker-Drob, E.M., Liewald, D.C., Hagenaars, S.P., Davies, G.,  
506 Wardlaw, J.M., Gale, C.R., Bastin, M.E., and Deary, I.J. (2016). Ageing and brain white  
507 matter structure in 3,513 UK Biobank participants. *Nat Commun* 7, 13629.
- 508 Dahnke, R., Ziegler, G., and Gaser, C. (2019). Detection of White Matter Hyperintensities in  
509 T1 without FLAIR. In *Human Brain Mapping Conference (Rome)*.
- 510 Davis, S.W., Dennis, N.A., Buchler, N.G., White, L.E., Madden, D.J., and Cabeza, R. (2009).  
511 Assessing the effects of age on long white matter tracts using diffusion tensor tractography.  
512 *Neuroimage* 46, 530-541.
- 513 de Bruijn, R.F., and Ikram, M.A. (2014). Cardiovascular risk factors and future risk of  
514 Alzheimer's disease. *BMC Med* 12, 130.
- 515 de Groot, J.C., de Leeuw, F.E., Oudkerk, M., van Gijn, J., Hofman, A., Jolles, J., and  
516 Breteler, M.M. (2000). Cerebral white matter lesions and cognitive function: the Rotterdam  
517 Scan Study. *Ann Neurol* 47, 145-151.
- 518 de Leeuw, F.E., de Groot, J.C., Achten, E., Oudkerk, M., Ramos, L.M., Heijboer, R., Hofman,  
519 A., Jolles, J., van Gijn, J., and Breteler, M.M. (2001). Prevalence of cerebral white matter  
520 lesions in elderly people: a population based magnetic resonance imaging study. The  
521 Rotterdam Scan Study. *J Neurol Neurosurg Psychiatry* 70, 9-14.
- 522 Debette, S., and Markus, H.S. (2010). The clinical importance of white matter  
523 hyperintensities on brain magnetic resonance imaging: systematic review and meta-analysis.  
524 *BMJ* 341, c3666.
- 525 Dobbins, I.G., Foley, H., Schacter, D.L., and Wagner, A.D. (2002). Executive control during  
526 episodic retrieval: multiple prefrontal processes subserving source memory. *Neuron* 35, 989-  
527 996.
- 528 Fazekas, F., Chawluk, J.B., Alavi, A., Hurtig, H.I., and Zimmerman, R.A. (1987). MR signal  
529 abnormalities at 1.5 T in Alzheimer's dementia and normal aging. *AJR Am J Roentgenol* 149,  
530 351-356.

531 Felsenstein, O., Peled, N., Hahn, E., Rockhill, A.P., Folsom, L., Gholipour, T., Macadams, K.,  
532 Rozengard, N., Paulk, A.C., Dougherty, D., *et al.* (2019). Multi-Modal Neuroimaging Analysis  
533 and Visualization Tool (MMVT) (arXiv).

534 Fox, J., and Weisberg, S. (2019). An R companion to applied regression, Third edition. edn.  
535 Garo-Pascual, M., Gaser, C., Zhang, L., Tohka, J., Medina, M., and Strange, B.A. (2023).  
536 Brain structure and phenotypic profile of superagers compared with age-matched older  
537 adults: a longitudinal analysis from the Vallecas Project. *Lancet Healthy Longev.*

538 Gefen, T., Peterson, M., Papastefan, S.T., Martersteck, A., Whitney, K., Rademaker, A.,  
539 Bigio, E.H., Weintraub, S., Rogalski, E., Mesulam, M.M., *et al.* (2015). Morphometric and  
540 histologic substrates of cingulate integrity in elders with exceptional memory capacity. *The*  
541 *Journal of neuroscience* *35*, 1781-1791.

542 Glisky, E.L. (2007). *Changes in Cognitive Function in Human Aging* (CRC Press/Taylor &  
543 Francis).

544 Goldstein, F.C., Mao, H., Wang, L., Ni, C., Lah, J.J., and Levey, A.I. (2009). White Matter  
545 Integrity and Episodic Memory Performance in Mild Cognitive Impairment: A Diffusion Tensor  
546 Imaging Study. *Brain Imaging Behav* *3*, 132-141.

547 Haller, S., Kovari, E., Herrmann, F.R., Cuvinciuc, V., Tomm, A.M., Zulian, G.B., Lovblad,  
548 K.O., Giannakopoulos, P., and Bouras, C. (2013). Do brain T2/FLAIR white matter  
549 hyperintensities correspond to myelin loss in normal aging? A radiologic-neuropathologic  
550 correlation study. *Acta Neuropathol Commun* *1*, 14.

551 Harrison, T.M., Maass, A., Baker, S.L., and Jagust, W.J. (2018). Brain morphology,  
552 cognition, and  $\beta$ -amyloid in older adults with superior memory performance. *Neurobiology of*  
553 *Aging* *67*, 162-170.

554 Harrison, T.M., Weintraub, S., Mesulam, M.M., and Rogalski, E. (2012). Superior memory  
555 and higher cortical volumes in unusually successful cognitive aging. *Journal of the*  
556 *International Neuropsychological Society* *18*, 1081-1085.

557 Hua, K., Zhang, J., Wakana, S., Jiang, H., Li, X., Reich, D.S., Calabresi, P.A., Pekar, J.J.,  
558 van Zijl, P.C., and Mori, S. (2008). Tract probability maps in stereotaxic spaces: analyses of  
559 white matter anatomy and tract-specific quantification. *Neuroimage* *39*, 336-347.

560 Ingo, C., Kurian, S., Higgins, J., Mahinrad, S., Jenkins, L., Gorelick, P., Lloyd-Jones, D., and  
561 Sorond, F. (2021). Vascular health and diffusion properties of normal appearing white matter  
562 in midlife. *Brain Commun* *3*, fcab080.

563 Jenkinson, M., Beckmann, C.F., Behrens, T.E., Woolrich, M.W., and Smith, S.M. (2012). *Fsl.*  
564 *Neuroimage* *62*, 782-790.

565 Kennedy, K.M., and Raz, N. (2009). Aging white matter and cognition: differential effects of  
566 regional variations in diffusion properties on memory, executive functions, and speed.  
567 *Neuropsychologia* *47*, 916-927.

568 Kim, B.R., Kwon, H., Chun, M.Y., Park, K.D., Lim, S.M., Jeong, J.H., and Kim, G.H. (2020).  
569 White Matter Integrity Is Associated With the Amount of Physical Activity in Older Adults With  
570 Super-aging. *Frontiers in Aging Neuroscience* *12*, 549983-549983.

571 Kochunov, P., Thompson, P.M., Lancaster, J.L., Bartzokis, G., Smith, S., Coyle, T., Royall,  
572 D.R., Laird, A., and Fox, P.T. (2007). Relationship between white matter fractional anisotropy  
573 and other indices of cerebral health in normal aging: tract-based spatial statistics study of  
574 aging. *Neuroimage* *35*, 478-487.

575 Launer, L.J., Oudkerk, M., Nilsson, L.G., Alperovitch, A., Berger, K., Breteler, M.M., Fuhrer,  
576 R., Giampaoli, S., Nissinen, A., Pajak, A., *et al.* (2000). CASCADE: a European collaborative  
577 study on vascular determinants of brain lesions. Study design and objectives.  
578 *Neuroepidemiology* *19*, 113-120.

579 Lei, D., Ma, J., Shen, X., Du, X., Shen, G., Liu, W., Yan, X., and Li, G. (2012). Changes in  
580 the brain microstructure of children with primary monosymptomatic nocturnal enuresis: a  
581 diffusion tensor imaging study. *PLoS One* 7, e31023.

582 Lockhart, S.N., Mayda, A.B., Roach, A.E., Fletcher, E., Carmichael, O., Maillard, P.,  
583 Schwarz, C.G., Yonelinas, A.P., Ranganath, C., and Decarli, C. (2012). Episodic memory  
584 function is associated with multiple measures of white matter integrity in cognitive aging.  
585 *Front Hum Neurosci* 6, 56.

586 O'Sullivan, M., Jones, D.K., Summers, P.E., Morris, R.G., Williams, S.C., and Markus, H.S.  
587 (2001). Evidence for cortical "disconnection" as a mechanism of age-related cognitive  
588 decline. *Neurology* 57, 632-638.

589 Olazarán, J., Valentí, M., Belén, F., Zea-Sevilla, M.A., Ávila-Villanueva, M., Fernández-  
590 Blázquez, M.Á., Calero, M., Dobato, J.L., Hernández-Tamames, J.A., León-Salas, B., *et al.*  
591 (2015). The Vallecas Project: A cohort to identify early markers and mechanisms of  
592 Alzheimer's disease. *Frontiers in Aging Neuroscience* 7, 181.

593 Peña-Casanova, J., Gramunt-Fombuena, N., Quiñones-Úbeda, S., Sánchez-Benavides, G.,  
594 Aguilar, M., Badenes, D., Molinuevo, J.L., Robles, A., Barquero, M.S., Payno, M., *et al.*  
595 (2009). Spanish multicenter normative studies (NEURONORMA project): Norms for the rey-  
596 osterrieth complex figure (copy and memory), and free and cued selective reminding test.  
597 *Archives of Clinical Neuropsychology* 24, 371-393.

598 Pfefferbaum, A., Adalsteinsson, E., and Sullivan, E.V. (2005). Frontal circuitry degradation  
599 marks healthy adult aging: Evidence from diffusion tensor imaging. *Neuroimage* 26, 891-899.

600 Prins, N.D., and Scheltens, P. (2015). White matter hyperintensities, cognitive impairment  
601 and dementia: an update. *Nat Rev Neurol* 11, 157-165.

602 Raz, N. (2000). Aging of the brain and its impact on cognitive performance: Integration of  
603 structural and functional findings. In *The handbook of aging and cognition* (Mahwah, N.J.:  
604 Lawrence Erlbaum Associates), pp. ix, 755 p.

605 Sasson, E., Doniger, G.M., Pasternak, O., Tarrasch, R., and Assaf, Y. (2013). White matter  
606 correlates of cognitive domains in normal aging with diffusion tensor imaging. *Front Neurosci*  
607 7, 32.

608 Simons, J.S., and Spiers, H.J. (2003). Prefrontal and medial temporal lobe interactions in  
609 long-term memory. *Nature Reviews Neuroscience* 4, 637-648.

610 Slater, D.A., Melie-Garcia, L., Preisig, M., Kherif, F., Lutti, A., and Draganski, B. (2019).  
611 Evolution of white matter tract microstructure across the life span. *Hum Brain Mapp* 40,  
612 2252-2268.

613 Smith, S.M., Jenkinson, M., Johansen-Berg, H., Rueckert, D., Nichols, T.E., Mackay, C.E.,  
614 Watkins, K.E., Ciccarelli, O., Cader, M.Z., Matthews, P.M., *et al.* (2006). Tract-based spatial  
615 statistics: voxelwise analysis of multi-subject diffusion data. *Neuroimage* 31, 1487-1505.

616 Song, S.K., Sun, S.W., Ju, W.K., Lin, S.J., Cross, A.H., and Neufeld, A.H. (2003). Diffusion  
617 tensor imaging detects and differentiates axon and myelin degeneration in mouse optic nerve  
618 after retinal ischemia. *Neuroimage* 20, 1714-1722.

619 Song, S.K., Yoshino, J., Le, T.Q., Lin, S.J., Sun, S.W., Cross, A.H., and Armstrong, R.C.  
620 (2005). Demyelination increases radial diffusivity in corpus callosum of mouse brain.  
621 *Neuroimage* 26, 132-140.

622 Sullivan, E.V., and Pfefferbaum, A. (2006). Diffusion tensor imaging and aging. *Neurosci*  
623 *Biobehav Rev* 30, 749-761.

624 Sun, F.W., Stepanovic, M.R., Andreano, J., Barrett, L.F., Touroutoglou, A., and Dickerson,  
625 B.C. (2016). Youthful Brains in Older Adults: Preserved Neuroanatomy in the Default Mode  
626 and Salience Networks Contributes to Youthful Memory in Superaging. *Journal of*  
627 *Neuroscience* 36, 9659-9668.



628 Szczepanski, S.M., and Knight, R.T. (2014). Insights into human behavior from lesions to the  
629 prefrontal cortex. *Neuron* 83, 1002-1018.

630 Tomita, H., Ohbayashi, M., Nakahara, K., Hasegawa, I., and Miyashita, Y. (1999). Top-down  
631 signal from prefrontal cortex in executive control of memory retrieval. *Nature* 401, 699-703.

632 Tubi, M.A., Feingold, F.W., Kothapalli, D., Hare, E.T., King, K.S., Thompson, P.M., Braskie,  
633 M.N., and Alzheimer's Disease Neuroimaging, I. (2020). White matter hyperintensities and  
634 their relationship to cognition: Effects of segmentation algorithm. *Neuroimage* 206, 116327.

635 Valdes Hernandez Mdel, C., Morris, Z., Dickie, D.A., Royle, N.A., Munoz Maniega, S.,  
636 Aribisala, B.S., Bastin, M.E., Deary, I.J., and Wardlaw, J.M. (2013). Close correlation  
637 between quantitative and qualitative assessments of white matter lesions.  
638 *Neuroepidemiology* 40, 13-22.

639 van Straaten, E.C., Fazekas, F., Rostrup, E., Scheltens, P., Schmidt, R., Pantoni, L., Inzitari,  
640 D., Waldemar, G., Erkinjuntti, T., Mantyla, R., *et al.* (2006). Impact of white matter  
641 hyperintensities scoring method on correlations with clinical data: the LADIS study. *Stroke*  
642 37, 836-840.

643 Wakana, S., Caprihan, A., Panzenboeck, M.M., Fallon, J.H., Perry, M., Gollub, R.L., Hua, K.,  
644 Zhang, J., Jiang, H., Dubey, P., *et al.* (2007). Reproducibility of quantitative tractography  
645 methods applied to cerebral white matter. *Neuroimage* 36, 630-644.

646 Westlye, L.T., Walhovd, K.B., Dale, A.M., Bjornerud, A., Due-Tonnessen, P., Engvig, A.,  
647 Grydeland, H., Tamnes, C.K., Ostby, Y., and Fjell, A.M. (2010). Life-span changes of the  
648 human brain white matter: diffusion tensor imaging (DTI) and volumetry. *Cereb Cortex* 20,  
649 2055-2068.

650 Ylikoski, A., Erkinjuntti, T., Raininko, R., Sarna, S., Sulkava, R., and Tilvis, R. (1995). White  
651 matter hyperintensities on MRI in the neurologically nondiseased elderly. Analysis of cohorts  
652 of consecutive subjects aged 55 to 85 years living at home. *Stroke* 26, 1171-1177.

653 Ziegler, D.A., Piguet, O., Salat, D.H., Prince, K., Connally, E., and Corkin, S. (2010).  
654 Cognition in healthy aging is related to regional white matter integrity, but not cortical  
655 thickness. *Neurobiol Aging* 31, 1912-1926.

656

657

658 **TABLES**

659 **Table 1. Demographic and cross-sectional white matter volume and white matter lesion**  
660 **differences between superagers and typical older adults.** Volumetric group differences  
661 were calculated with total intracranial volume included as a covariate. The mean and standard  
662 deviation (SD) reported in the table correspond to raw values. Group differences in the  
663 Fazekas scale were assessed with a Chi-square test and Fisher's exact test. See Extended  
664 Data Table 1-1 for the longitudinal evolution of the neuropsychological variables. FDR  $P$ , False  
665 Discovery Rate  $p$ -value;  $P$ ,  $p$ -value.

JNeurosci Accepted Manuscript

	Superagers n = 64	Typical older adults n = 55	Statistic	P	FDR P
<i>Demographics</i>					
<b>Age</b> , mean (SD), years	81.9 (1.9)	82.4 (1.9)	Z = -1.8	0.08	0.15
<b>Female</b> , No. (%)	38 (59)	35 (64)	X = -0.1	0.77	0.85
<b>Education</b> , mean (SD), years	14.6 (6.0)	11.7 (7.2)	Z = 2.4	0.02	0.04
<i>Neuropsychological selection criteria variables</i>					
<b>Free and Cued Selective Reminding Test free delayed recall score</b> , mean (SD)	13.4 (1.4)	6.5 (1.6)	Z = 9.4	<2x10 <sup>-16</sup>	2x10 <sup>-15</sup>
<b>Animal Fluency Test total score</b> , mean (SD)	21.2 (4.8)	15.9 (4.1)	t = 6.5	2x10 <sup>-9</sup>	1x10 <sup>-8</sup>
<b>Digit Symbol Substitution Test total score</b> , mean (SD)	21.2 (6.1)	15.3 (5.8)	t = 5.4	4x10 <sup>-7</sup>	1x10 <sup>-6</sup>
<b>15-item Boston Naming Test total score</b> , mean (SD)	13.8 (1.4)	11.5 (2.5)	Z = 5.4	7x10 <sup>-8</sup>	3x10 <sup>-7</sup>
<i>White matter structure</i>					
<b>White matter volume</b> , mean (SD), cm <sup>3</sup>	441.80 (54.99)	439.08 (55.46)	F = 0.4	0.54	0.66
<b>White matter lesions volume</b> , mean (SD), cm <sup>3</sup>	3.28 (3.32)	4.52 (6.35)	F = 1.9	0.17	0.27
<b>White matter lesion presence vs. absence</b> on Fazekas scoring, No. (%)	55 (85.9)	45 (83.3)	χ = 0.02	0.89	0.89
<b>Fazekas score</b> , 1	35 (63.6)	24 (53.3)	Fisher's Exact Test	0.45	0.62
No. (%) 2	17 (30.9)	16 (35.6)			
3	3 (5.5)	5 (11.1)			

## FIGURE'S LEGEND

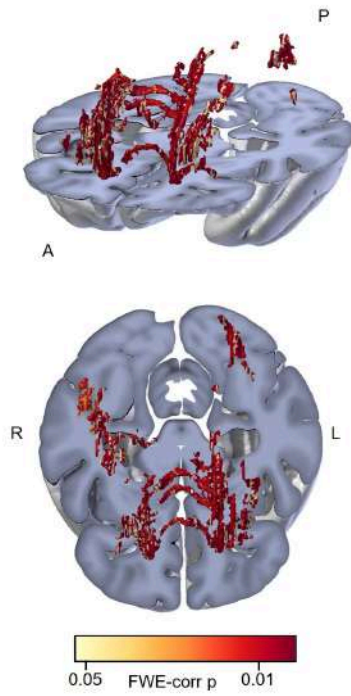
**Figure 1. Better white matter microstructure in superagers, particularly in frontal white matter tracts, compared to typical older adults. A.** Superagers show higher fractional anisotropy than typical older adults in bilateral frontal tracts and the anterior thalamic radiation (warm colours,  $P < 0.05$  FWE-corrected). **B.** Lower mean diffusivity (MD) is found in superagers compared to typical older adults in an extensive network (cold colours,  $P < 0.05$  FWE-corrected). **C.** Significantly greater MD group differences in the anterior half of the brain as indicated by the linear fit (blue line) of the parameter estimates ( $\beta$ ) of the contrast MD higher in typical older adults than in superagers as a function of anteroposterior axis coordinates (positive Montreal Neurologic Initiative (MNI) coordinates for the anterior portion of the brain). See Extended Data Figure 1-1 for the correlation between FA and MD values and episodic memory performance and Figure 1-2 for group differences in additional diffusivity measures. Mean  $\beta$  and  $\pm$  standard error are plotted. A, anterior; L, left; R, right; P, posterior; FWE-corr p, family-wise corrected  $p$ -value.

**Figure 2. Longitudinal evolution of white matter volume and white matter lesions volume in superagers and typical older adults. A.** Predicted trajectories of total brain white matter volume over time were plotted for superagers (red line) and typical older adults (blue line) with respective shaded areas indicating the 95% confidence interval and individual trajectories in black, showing no difference at baseline or atrophy rate between groups. **B.** Accumulation over time of white matter lesions measured as white matter lesion volume. There was no baseline difference between groups and longitudinal trajectories between groups were no longer significantly different after exclusion of outliers, three typical older adults and a superager indicated in grey. White matter volumes and white matter lesion volumes have been adjusted by total intracranial volume in the statistical model and for illustration purposes. Age was scaled in the statistical model, but raw values are shown for illustration purposes. See Extended Data Figure 2-1 for further details of the statistical models.

**Figure 3. Longitudinal changes in diffusivity measures between superagers and typical older adults.** **A.** Longitudinal differences in fractional anisotropy. Superagers show a slower decrease of fractional anisotropy compared to typical older adults in an extended network of white matter tracts (shaded regions) ( $P < 0.05$  FWE-corrected). See Extended Data Figures 3-1 and 3-2 for ROI-based analyses. **B.** Longitudinal differences in mean diffusivity. Superagers show a slower increase of mean diffusivity compared to typical older adults in an extended network of white matter tracts (shaded regions) ( $P < 0.05$  FWE-corrected). See Extended Data Figures 3-3 and 3-4 for ROI-based analyses. **C.** JHU-ICBM atlas labels of white matter tracts were used to map the significant effects shown in the rest of the panels. Note that the significant effects shown in A. and B. are not constrained to white matter since the fractional anisotropy and mean diffusivity maps were not limited to white matter skeleton. FWE-corr  $p$ , family-wise error  $p$ -value.

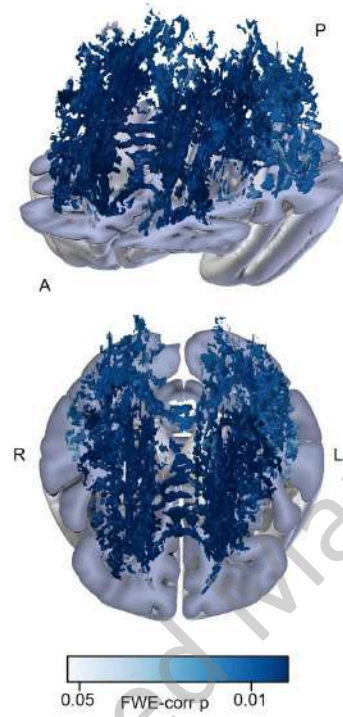
### A Fractional anisotropy

Superagers > Typical older adults



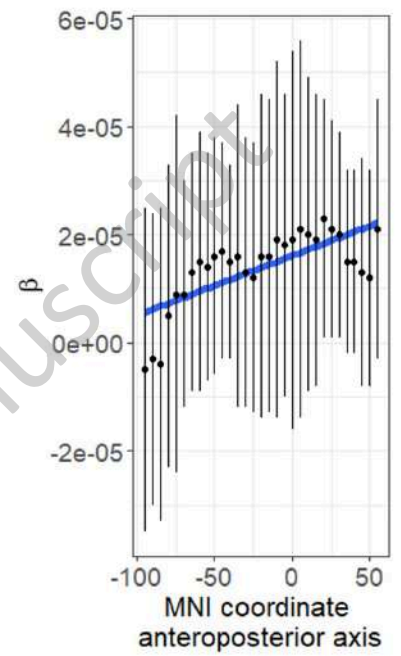
### B Mean diffusivity

Typical older adults > Superagers

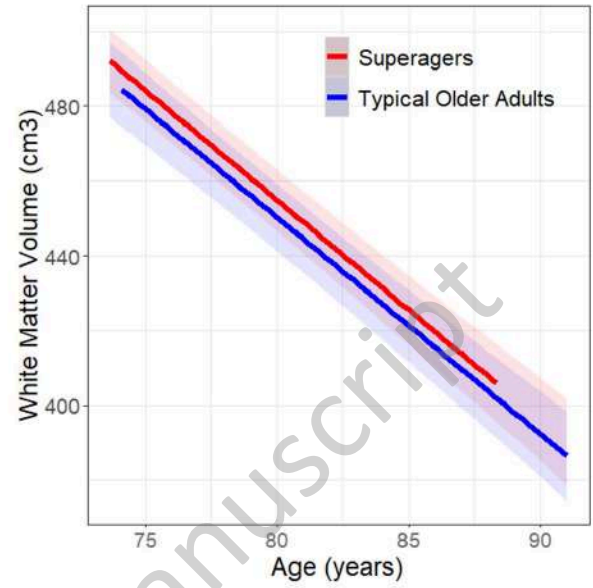
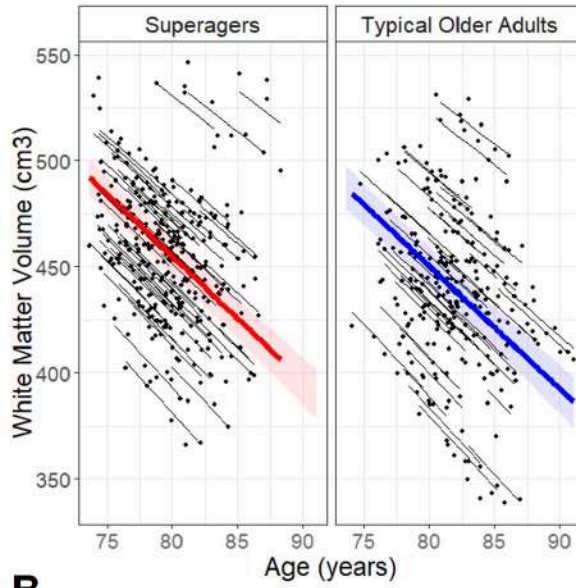


### C Parameter estimates ( $\beta$ ) mean diffusivity

Typical older adults > Superagers



JNeurosci Accepted Manuscript

**A****B**